Vietnam Journal of Catalysis and Adsorption
Tạp chí xúc tác và hấp phụ Việt Nam

https://jca.edu.vn

Unveiling the electronic and optical properties of $(TiO_2)_7$ cluster supported on Fe-MIL-88B: A Theoretical Insight

Ngo Hoang Lan[1], Vu Thi Huong[1], Bui Cong Trinh[2], Nguyen Ngoc Ha[1], Nguyen Thi Thu Ha[1,*]

[1] *Faculty of Chemistry, Hanoi National University of Education, 136 Xuan Thuy, Cau Giay, Hanoi, Vietnam*
[2] *Institute for Technology of Radioactive and Rare Elements, 48 Lang Ha, Dong Da, Hanoi, Vietnam*
** Email: ntt.ha@hnue.edu.vn*

ARTICLE INFO

Received: 29/09/2024
Accepted: 24/11/2024
Published: 30/03/2025

Keywords: TiO_2; Fe-MIL-88B, GFN1-xTB; photocatalyst.

ABSTRACT

This study investigates the structural, electronic, and optical properties of a composite material system composed of the $(TiO_2)_7$ cluster and Fe-MIL-88B. The structural optimization and interaction energy calculations were performed using the GFN1-xTB method. The interaction between TiO_2 and Fe-MIL-88B is quantified through these calculations, revealing a thermodynamically favorable formation with an interaction energy of -199.54 kJ mol^{-1}. Bond order analysis and interatomic distances indicate weak chemical bonding between Ti and C atoms, further supported by a total bond order of 0.746. The electronic properties, including ionization potential (IP), electron affinity (EA), and global electrophilicity index (GEI), were computed, showing that the TiO_2/Fe-MIL-88B composite exhibits enhanced electron-accepting behavior. UV-Vis spectral analysis and band gap calculations reveal that the composite demonstrates a reduced band gap compared to its individual components, facilitating better electron-hole separation and charge transfer. The findings highlight the potential of the TiO_2/Fe-MIL-88B composite for photocatalytic applications, offering valuable insights into the development of hybrid materials for environmental remediation and renewable energy production.

Introduction

The rising concentration of carbon dioxide (CO_2) in the atmosphere has led to significant environmental changes, directly impacting human health and daily life. Extensive scientific research has been undertaken to reduce CO_2 emissions into the atmosphere. These efforts have largely focused on two approaches: i) CO_2 capture and storage (CCS) technology [1], and ii) the conversion of CO_2 into valuable products [2]. The latter approach is seen as particularly promising, as CO_2 can be utilized as a carbon source. In industrial applications, CO_2 is widely employed in both the Sabatier reaction and the reverse water-gas shift (RWGS) reaction. In the Sabatier reaction, CO_2 reacts with H_2 to produce CH_4 and H_2O at temperatures between 300 and 400**℃** [3,4]. For the RWGS reaction, CO_2 first reacts with H_2 to form CO and H_2O, with the CO subsequently being converted into hydrocarbons via the Fischer-Tropsch process [5,6]. However, both reactions require high temperatures and pressures. This underscores the need for the development of alternative CO_2 reduction methods that are energy-efficient, cost-effective, and environmentally sustainable.

The development of renewable energy, particularly solar energy, has gained significant attention as a solution to the energy crisis and environmental

https://doi.org/10.62239/jca.2025.004

challenges [7], with photocatalytic CO_2 reduction processes like artificial photosynthesis emerging as a promising approach for converting CO_2 into fuels or valuable organic compounds using solar energy and water. Common photocatalysts employed in CO_2 conversion include semiconductor oxides such as TiO_2, ZnO, CeO_2, ZrO_2, Fe_2O_3 and WO_3 [8-13]. Among these, TiO_2, one of the most widely studied semiconductors, remains a focal point of research. However, due to its large bandgap energy (3.2 eV) and the high recombination rate of photogenerated electrons (e*) and holes (h^+), the efficiency of TiO_2 in photocatalytic CO_2 conversion remains limited [8].

In recent years, metal-organic frameworks (MOFs) have emerged as promising photocatalytic materials, attracting significant attention for their unique properties. These include a crystalline porous structure, a large specific surface area that facilitates CO_2 adsorption, and highly ordered, tunable chemical components, all of which contribute to enhancing the efficiency of photocatalytic processes. Combining traditional photocatalysts like TiO_2 with MOFs, such as Fe-MIL-88B, can significantly improve the efficiency of photocatalytic CO_2 conversion [14]. Fe-MIL-88B, an iron-based MOF, enhances the photocatalytic performance of TiO_2 by broadening its light absorption range from the ultraviolet (UV) to the visible spectrum, thereby increasing its overall photocatalytic activity. Additionally, the combination reduces the band gap of TiO_2, promoting more efficient charge separation and extending the lifetime of photogenerated electron-hole pairs [14,15]. The direct excitation of Fe–O clusters in Fe-MIL-88B triggers electron transfer from O^{2-} to Fe^{3+}, forming Fe^{2+}, which is responsible for the photocatalytic reduction of CO_2 [16].

Despite these promising results, there have been relatively few theoretical studies exploring the interaction between TiO_2 and Fe-MIL-88B. As a result, many of the underlying mechanisms that contribute to their enhanced photocatalytic performance remain unclear. Therefore, the objective of this study is to conduct theoretical calculations to elucidate the nature of the interaction between TiO_2 and Fe-MIL-88B, providing deeper insights into their synergistic effects and potential for improving CO_2 photoreduction efficiency.

Models and computational methods

Models

The $(TiO_2)_7$ cluster was selected for this research due to its superior stability in comparison to other small $(TiO_2)_n$ clusters (n = 1–9), based on the calculated formation energy per TiO_2 unit [17]. The initial geometry of this cluster was modeled after the anatase phase of bulk TiO_2. A Fe-MIL-88B structure similar to those used in previous study from our group was adopted [18]. This MOF framework consists of octahedral μ_3-Fe_3O clusters connected through benzene-1,4-dicarboxylate (BDC) linkers, forming a hexagonal array of aligned, corner-sharing trigonal prisms. The resulting structure forms a three-dimensional hexagonal network with P63/mmc space group symmetry. The choice of the $(TiO_2)_7$ cluster allowed for a practical balance between computational efficiency and structural accuracy, as smaller clusters are useful for exploring key interaction mechanisms. The Fe-MIL-88B model, with its stable structure and well-defined pore system, was utilized to mimic realistic adsorption and photocatalytic behavior, providing a solid basis for investigating the molecular-level interaction between TiO_2 and Fe-MIL-88B in the context of CO_2 photoreduction.

Computational methods

All structural optimizations and energy calculations were performed using the GFN1-xTB method, a semi-empirical tight-binding approach [19]. GFN1-xTB was selected for its computational efficiency and ability to handle a wide range of molecular systems with reasonable accuracy, particularly in comparison to more computationally expensive methods like density functional theory (DFT). The method is especially advantageous when studying large, complex systems due to its significantly lower computational cost, while still providing reliable predictions for geometries and electronic properties. GFN1-xTB has been successfully applied to similar systems involving metal-organic frameworks (MOFs) and transition-metal oxides [20, 21], making it well-suited for investigating the interaction between TiO_2 clusters and Fe-MIL-88B in this study. Its ability to optimize structures and calculate energetics in a resource-efficient manner allows for the exploration of various configurations and adsorption behaviors without compromising on accuracy. The electronic properties of the studied systems were further elucidated by evaluating parameters such as vertical ionization potential (IP), vertical electron affinity (EA), and Global Electrophilicity Index (GEI).

UV-Vis spectra were computed using the ultra-fast method for electronic spectra of large systems based on the tight-binding simplified Tamm-Dancoff approximation (sTDA) [22]. This approach was selected

https://doi.org/10.62239/jca.2025.004

due to its ability to efficiently handle large molecular systems while maintaining reasonable accuracy in predicting electronic transitions. The method provides a significant speed advantage over conventional time-dependent density functional theory (TD-DFT) while still offering reliable spectral data, making it well-suited for large-scale simulations.

Results and discussion

Interaction between TiO_2 and FeMIL-88B

Figure 1 below illustrates the optimized structure of the material system composed of the $(TiO_2)_7$ cluster and Fe-MIL-88B. The interaction between Fe-MIL-88B and the $(TiO_2)_7$ cluster is quantified by the interaction energy (E_{int}), which is calculated as follows:

$$E_{int} = E(TiO_2/\text{Fe-MIL-88B}) - E(\text{Fe-MIL-88B}) - E(TiO_2) \quad \text{(Eq.1)}$$

where $E(TiO_2/\text{Fe-MIL-88B})$, $E(\text{Fe-MIL-88B})$, and $E(TiO_2)$ are energy of TiO_2/Fe-MIL-88B, Fe-MIL-88B and TiO_2 cluster, respectively.

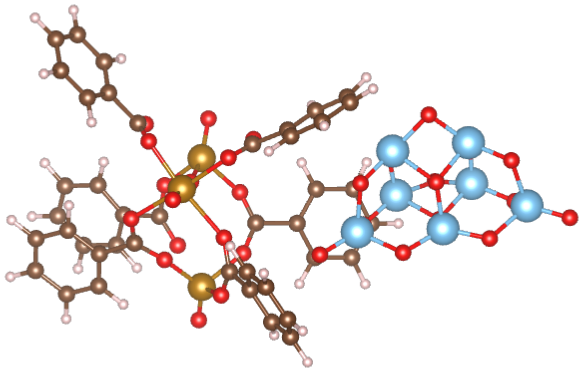

Figure 1: Optimized structure of $(TiO_2)_7$/Fe-MIL-88B. Color codes: brown – C, red – O, ivory – H, yellow brown – Fe, light blue – Ti

The interaction energy for the $(TiO_2)_7$/Fe-MIL-88B system was found to be -199.54 kJ mol^{-1}, indicating that the formation of this hybrid system is thermodynamically favorable. To further explore the interaction between Fe-MIL-88B and the $(TiO_2)_7$ cluster, we examined the Wiberg bond order (BO) and interatomic distances (d). The results show that the bond order between the Ti atoms of the $(TiO_2)_7$ cluster and the nearest C atoms of Fe-MIL-88B ranges from 0.143 to 0.225, with a total bond order of 0.746. This calculated bond order, based on the classical Wiberg indices, is slightly lower than the standard value of 1 for a typical single bond, indicating the presence of a weak bonding interaction. The shortest distance between Ti and Fe-MIL-88B corresponds to a Ti–C distance of 2.508 Å, which exceeds the sum of their atomic radii (2.1 Å). This is consistent with the low bond order values, where the bonds between Ti and C are less than 1. These findings suggest that the interaction between the $(TiO_2)_7$ cluster and Fe-MIL-88B is not purely physical but has a partial chemical nature. This is a crucial observation, as the formation of weak chemical bonds in the TiO_2/Fe-MIL-88B composite system can significantly influence the electronic structure and optical properties of the material, setting it apart from its individual components.

Electronic properties

The electronic properties of Fe-MIL-88B, $(TiO_2)_7$, and their composite system, as presented in Table 1, reveal significant insights into their photocatalytic potential.

Table 1. Calculated electronic properties of the studied systems

Parameter	$(TiO_2)_7$	Fe-MIL-88B	$(TiO_2)_7$/Fe-MIL-88B
IP, eV	11.403	8.530	8.640
EA, eV	4.532	5.127	5.505
GEI, eV	4.620	6.850	7.978

The ionization potential of the $(TiO_2)_7$ cluster is the highest at 11.403 eV, indicating a strong resistance to electron loss, while Fe-MIL-88B has a lower IP of 8.530 eV, which slightly increases to 8.640 eV in the composite, suggesting that the combination modifies the electronic structure. Electron affinity, which measures the ability to accept electrons, increases in the composite system (5.505 eV) compared to both the $(TiO_2)_7$ cluster (4.532 eV) and Fe-MIL-88B (5.127 eV), indicating enhanced electron-accepting capabilities. This increase in EA is beneficial for photocatalytic applications as it improves electron capture and reduces electron-hole recombination. Furthermore, the global electrophilicity index, which correlates with Lewis acidity, is significantly higher in the composite (7.978 eV) compared to its individual components, suggesting greater Lewis acidity and stronger electron-accepting behavior. These enhanced electronic properties, particularly the increased GEI and EA, suggest that the TiO_2/Fe-MIL-88B composite is more effective in photocatalytic processes like CO_2 reduction, where strong electron-accepting capabilities are essential for interacting with reactants and facilitating conversion reactions.

https://doi.org/10.62239/jca.2025.004

Optical properties

To compare and predict the photocatalytic activity of the materials, we calculated the UV-Vis spectra and band gap values. A key factor in explaining photocatalytic performance is determining the potential energies of the valence band (E_{VB}) and conduction band (E_{CB}). These potential energies are calculated using the absolute electronegativity (χ) and the energy of a free electron on the standard hydrogen electrode scale (E_e), based on the following formula:

$$\chi = \frac{IP+EA}{2} \quad \text{(Eq.2)}$$

$$E_{VB} = \chi - E_e + 0,5.E_g \quad \text{(Eq.3)}$$

$$E_{CB} = E_{VB} - E_g \quad \text{(Eq.4)}$$

where E_e = 4.5000 eV [23]

Figure 2 presents the UV-Vis spectra for the $(TiO_2)_7$ cluster, Fe-MIL-88B, and the TiO_2/Fe-MIL-88B composite. The calculated values for electronegativity (χ), band gap, conduction band energy (E_{CB}), and valence band energy (E_{VB}) are provided in Table 2.

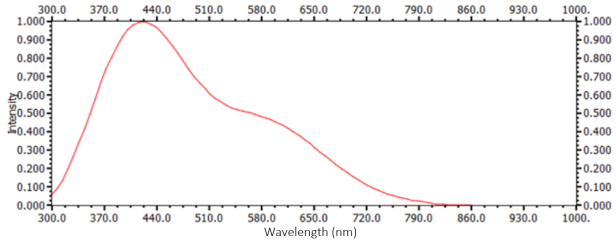

$(TiO_2)_7$

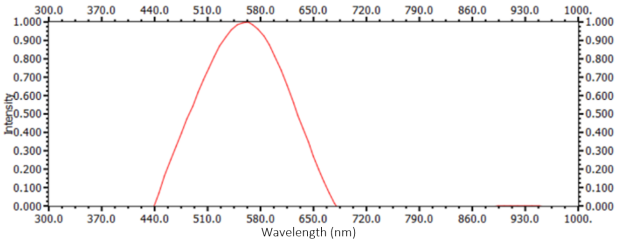

Fe-MIL-88B

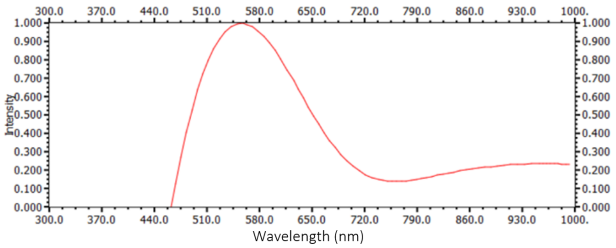

$(TiO_2)_7$/Fe-MIL-88B

Figure 2. Calculated spectrum of $(TiO_2)_7$, Fe-MIL-88B and $(TiO_2)_7$/Fe-MIL-88B

Table 2. Calculated absolute electronegativity, conduction band energy, and valence band energy

System	χ, eV	E_g, eV	E_{CB}, eV	E_{VB}, eV
$(TiO_2)_7$	7.9675	4.593	1.171	5.764
Fe-MIL-88B	6.8285	3.631	0.513	4.144
$(TiO_2)_7$/Fe-MIL-88B	7.0725	3.113	1.016	4.129

When TiO_2 is supported on Fe-MIL-88B, the UV-Vis absorption spectra (Figure 2) demonstrates a redshift, enhancing its absorption within the visible light region of $(TiO_2)_7$. Meanwhile, the absence of significant shifts in absorption peaks compared to Fe-MIL-88B indicates that the combination preserves the intrinsic light absorption characteristics of the MOF component. However, a more detailed analysis of the electronic properties, such as the band gap (E_g), conduction band energy (E_{CB}), and valence band energy (E_{VB}), reveals important trends. According to Table 2, the band gap of the TiO_2/Fe-MIL-88B composite (3.113 eV) is smaller than that of both the $(TiO_2)_7$ cluster (4.593 eV) and Fe-MIL-88B (3.631 eV), indicating enhanced electron-hole separation. The E_{CB} of the composite is calculated at 1.016 eV, lower than that of the $(TiO_2)_7$ cluster (1.171 eV), while the E_{VB} is also reduced to 4.129 eV, approaching the value for Fe-MIL-88B (4.144 eV). These changes in the energy levels suggest that the composite may facilitate improved charge transfer, which is crucial for photocatalytic processes like CO_2 reduction. It is important to note that the calculated band gaps are higher than those observed in bulk materials, primarily due to quantum confinement effects associated with the small system size [24]. However, the key observation here is the trend: the reduction in the band gap and slight lowering of the ECB indicate that the TiO_2/Fe-MIL-88B composite may be better suited for CO_2 photoreduction by promoting more efficient electron transfer, which is essential for converting CO_2 into useful products.

Conclusion

The interaction between the $(TiO_2)_7$ cluster and Fe-MIL-88B forms a thermodynamically stable hybrid system, as evidenced by the favorable interaction energy. Analysis of bond order and interatomic distances reveals weak but notable chemical interactions between TiO_2 and Fe-MIL-88B, which play a crucial role in modifying the electronic structure of the composite. This interaction enhances the electron

https://doi.org/10.62239/jca.2025.004

affinity and global electrophilicity index (GEI) of the system, indicating improved electron-accepting capabilities. Such properties are particularly advantageous for photocatalytic processes like CO_2 reduction, where efficient charge transfer is essential. Although the calculated band gaps are slightly higher due to quantum confinement effects, the overall reduction in the band gap and a lower conduction band energy level suggest a more effective mechanism for charge separation and transfer within the composite. These synergistic characteristics make the TiO_2/Fe-MIL-88B system a promising candidate for photocatalytic CO_2 reduction, offering a potential pathway to address environmental challenges and advance sustainable energy solutions..

Acknowledgments

This research is funded by Vietnam National Foundation for Science and Technology Development (NAFOSTED) under grant number of 104.06–2020.48. Ngo Hoang Lan was funded by Vingroup Joint Stock Company and supported by the Domestic Master/PhD Scholarship Program of Vingroup Innovation Foundation (VinIF), Vingroup Big Data Institute (VINBIGDATA), code VINIF.2021.TS.163.

References

1. R.S. Haszeldine, Science 325(5948) (2009) 1647–1652. http://doi.org/10.1126/science.1172246
2. G. Zhao, X. Huang, X. Wang, X. Wang, J. Mater. Chem. A 5(41) (2017) 21625–21649. https://doi.org/10.1039/C7TA07290B
3. Daza Y A, Kent R A, Yung M M, Kuhn J N, Ind Eng Chem Res, 53(14) (2014) 5828–5837. https://doi.org/10.1021/ie5002185
4. K.R. Thampi, J. Kiwi, M. Gratzel, Nature, 327 (1987) 506–508. https://doi.org/10.1038/327506a0
5. F. Bustamante, R. M. Enick, A.V. Cugini, R. P. Killmeyer, B. H. Howard, K. S. Rothenberger, M. V. Ciocco, B. D. Morreale, S. Chattopadhyay, S. Shi, AIChE Journal, 50(5) (2004) 1028-1041. https://doi.org/10.1002/aic.10099
6. Noji T, Jin T, Nango M, Kamiya N, et al, (2017), ACS Appl. Mater. Interfaces 2017, 9, 4, 3260–3265. https://doi.org/10.1021/acsami.6b12744
7. F.V. Bekun, A.A. Alola, S.A. Sarkodie, Sci. Total Environ. 657 (2019) 1023–1029. https://doi.org/10.1016/j.scitotenv.2018.12.104
8. N. Shehzad, M. Tahir, K. Johari, T. Murugesan, M. Hussain, et al., Journal of CO2 Utilization, 26 (2018) 98-122. https://doi.org/10.1016/j.jcou.2018.04.026
9. Z. Xiong, Z. Lei, Z. Xu, X. Chen, B. Gong, Y. Zhao, H. Zhao, J. Zhang, C. Zheng, Journal of CO_2 Utilization, 18 (2017) 53-61,. https://doi.org/10.1016/j.jcou.2017.01.013
10. T. Ohno, N. Murakami, T. Koyanagi, Y. Yang, Journal of CO_2 Utilization, 6 (2014) 17-25. https://doi.org/10.1016/j.jcou.2014.02.002
11. Y. Wang, B. Li, C. Zhang, L. Cui, S. Kang, X. Li, L. Zhou, Catalysis B: Environmental, Volumes 130–131 (2013) 277-284. http://doi.org/10.1016/j.apcatb.2012.11.019
12. C.C. Lo, C.H. Hung, C.S. Yuan, J.F. Wu , Solar Energy Materials and Solar Cells, 91(19) (2007) 1765-1774. https://doi.org/10.1016/j.solmat.2007.06.003
13. M. Mishra, D.M. Chun, Catalysis A: General, 498 (2015) 126-141. https://doi.org/10.1016/j.apcata.2015.03.023
14. P.T. Lan, N.H. Hao, N.V. Thuc, N.N. Ha, L.M. Cam, N.T.T. Ha, VNU Journal of Science: Natural Sciences and Technology, 39(4) (2023) 46-56. https://doi.org/10.25073/2588-1140/vnunst.5597
15. D. Xiang, Z. Wang, J. Xu, H. Shen, X. Zhang, N. Liu, Catalysts. 14 (2024) 528. https://doi.org/10.3390/catal14080528
16. Wang, D., Huang, R., Liu, W., Sun, D., & Li, Z. (2014), ACS Catal. 2014, 4, 12, 4254–4260. https://doi.org/10.1021/cs501169t
17. A. Zheng-wang, G.J. Kroes, J. Phys. Chem. B, 110(18) (2006) 8998–9007. https://doi.org/10.1021/jp056607p
18. N.T.T. Ha, H.T. Thao, N.N. Ha, Journal of Molecular Graphics and Modelling, 112 (2022) 108124. https://doi.org/10.1016/j.jmgm.2022.108124
19. C. Bannwarth, E. Caldeweyher, S. Ehlert, A. Hansen, P. Pracht, J. Seibert, S. Spicher, S. Grimme, WIREs Computational Molecular Science, 11(2) (2020) e1493. https://doi.org/10.1002/wcms.1493
20. Vicent-Luna, J. M., Apergi, S., & Tao, S. J., Chem. Inf. Model, 61(9) (2021) 4415–4424. https://doi.org/10.1021/acs.jcim.1c00432
21. Nurhuda, M., Perry, C. C., & Addicoat, M. A., Physical Chemistry Chemical Physics, 24(18) (2022) 10906-10914. https://doi.org/10.1039/D2CP00184E
22. Grimme, S. and Bannwarth, C., J. Chem. Phys. 145 (2016) 054103. https://doi.org/10.1063/1.4959605
23. Morrison, S. Roy (Stanley Roy). Electrochemistry at Semiconductor and Oxidized Metal Electrodes. Plenum Press, 1980.
24. Oleg D. Neikov, Stanislav S. Naboychenko and Nikolay A. Yefimov, Handbook of Non-Ferrous Metal Powders: Technologies and Applications, Elsevier Press, Second Edition, 2019, 271-311.